Biochemical and Biophysical Research Communications 449 (2014) 399–404

Contents lists available at ScienceDirect

Biochemical and Biophysical Research Communications

journal homepage: www.elsevier.com/locate/ybbrc

Structural basis of the phosphorylation dependent complex formation of neurodegenerative disease protein Ataxin-1 and RBM17

Eunji Kim [a,1,2], Yoonji Lee [b,1], Sun Choi [b,*], Ji-Joon Song [a,*]

[a] Department of Biological Sciences, Korea Advanced Institute of Science and Technology (KAIST), Daejeon 305-701, Republic of Korea
[b] National Leading Research Laboratory (NLRL) of Molecular Modeling & Drug Design, College of Pharmacy, Graduate School of Pharmaceutical Sciences, and Global Top 5 Program, Ewha Womans University, Seoul 120-750, Republic of Korea

ARTICLE INFO

Article history:
Received 10 May 2014
Available online 22 May 2014

Keywords:
Neurodegenerative disease
Spinocerebellar Ataxia Type1 (SCA1)
Structure modeling
Interaction
Phosphorylation

ABSTRACT

Spinocerebellar Ataxia Type1 (SCA1) is a dominantly inherited neurodegenerative disease and belongs to polyglutamine expansion disorders. The polyglutamine expansion in Ataxin-1 (ATXN1) is responsible for SCA1 pathology. ATXN1 forms at least two distinct complexes with Capicua (CIC) or RNA-binding motif protein 17 (RBM17). The wild-type ATXN1 dominantly forms a complex with CIC and the polyglutamine expanded form of ATXN1 favors to form a complex with RBM17. The phosphorylation of Ser776 in ATXN1 is critical for SCA1 pathology and serves as a binding platform for RBM17. However, the molecular basis of the phospho-specific binging of ATXN1 to RBM17 is not delineated. Here, we present the modeled structure of RBM17 bound to the phosphorylated ATXN1 peptide. The structure reveals the phosphorylation specific interaction between ATXN1 and RBM17 through a salt-bridge network. Furthermore, the modeled structure and the interactions between RBM17 and ATXN1 were validated through mutagenesis study followed by Surface Plasmon Resonance binding experiments. This work delineates the molecular basis of the interaction between RBM17 and the phosphorylated form of ATXN1, which is critical for SCA1 pathology. Furthermore, the structure of RBM17 and pATXN1 peptide might be utilized to target RBM17–ATXN1 interaction to modulate SCA1 pathogenesis.

1. Introduction

Polyglutamine diseases are dominantly inherited neurodegenerative disorders caused by an expansion of the CAG (encoding glutamine)-trinucleotide repeat region in the disease-related genes. Nine polyglutamine diseases are so far known including Huntington's disease, dentatorubropallidoluysian atrophy, spinobulbar muscular atrophy, and six spinocerebellar ataxias types (SCA) [1]. The length of polyglutamine expansion is shown to be correlated with the age of disease onset and the disease severity [2]. Even though the polyglutamine expanded proteins are ubiquitously expressed in all cell types, pathogenesis occurs only in specific brain areas. While the mechanisms of pathogenesis are poorly understood, intranuclear and cytoplasmic aggregates containing the polyglutamine expanded protein are found in affected neurons in all polyglutamine diseases as a common hallmark of the diseases.

SCA1 is one of the nine polyglutamine expansion neurodegenerative diseases. A major pathological feature of SCA1 is selective loss of Purkinje cells in the cerebellar cortex leading to progressive loss of motor coordination, speech impairment and problems with swallowing and breathing, eventually causing death [3,4]. The polyglutamine expansion in Ataxin-1 (ATXN1) is responsible for SCA1 [5,6]. ATXN1 contains AXH domain at the middle, and a polyglutamine repeat at the N-terminal region of ATXN1. ATXN1 has several binding partners. In nucleus, ATXN1 forms at least two complexes: one containing transcriptional repressor CIC and the other containing RBM17. Wild-type (non-expanded form) ATXN1 prefers to form a complex with CIC, while polyglutamine expanded ATXN1 favors to form a complex with RBM17 [7]. However, both ATXN1–RBM17 and ATXN1–CIC complexes are implicated in SCA1 disease and the balance between these two complexes might be critical for SCA1 pathogenesis [8].

CIC is a transcription factor containing HMG-box domain and predominantly expressed during granule cell development in the cerebellum, hippocampus and olfactory bulb. CIC is involved in ErbB signaling and central nerve system (CNS) development [9,10]. The evolutionarily conserved N-terminal region of CIC interacts with the AXH domain of ATXN1, and the reduction of CIC protein level

* Corresponding authors. Fax: +82 2 3277 2851 (S. Choi), fax: +82 42 350 2610 (J.-J. Song).
E-mail addresses: sunchoi@ewha.ac.kr (S. Choi), songj@kaist.ac.kr (J.-J. Song).
[1] These authors contributed equally.
[2] Present address: Korea Institute of Science and Technology (KIST), Seoul 136-791, Republic of Korea.

http://dx.doi.org/10.1016/j.bbrc.2014.05.063
0006-291X/

partially rescues SCA1-like phenotype in a mouse model [11]. We recently determined the crystal structure of ATXN1 AXH domain bound to CIC and revealed that ATXN1 undergoes reconfiguration from homodimer to hetero-tetramer upon CIC binding [12].

RBM17, also known as SPF 45, is a part of the spliceosome complex regulating mRNA splicing and abundant in Purkinje cell nuclei [7,13]. RBM17 is shown to mediate the toxicity of polyglutamine expanded ATXN1 in *Drosophila* model of SCA1 [7]. It was shown that Retinal degeneration, ommatidial disorganization and fusion, and interommatidial bristle loss were worsened when polyglutamine expanded ATXN1 and RBM17 was co-expressed than wild-type ATXN1 and RBM17, which is consistent with that RBM17 preferentially interacts with polyglutamine expanded ATXN1 and that the interaction between ATXN1 and RBM17 is implicated with SCA1 pathology [7]. The phosphorylation of Ser776 of ATXN1 by MSK1 pathway serves a binding platform for RBM17. Furthermore, the Ser776 phosphorylation is critical for SCA1 pathology as well as for the stability of ATXN1 [7,14–16]. However, the biological consequence of the phosphorylation of ATXN1 leading to RBM17 complex formation is not clearly understood. Despite of the importance of RBM17–ATXN1 interactions in SCA1 pathology, molecular basis of the phosphorylation dependency of RBM17–ATXN1 interaction has not been delineated. Here, we present the structure of RBM17 bound to ATXN1 peptide by molecular modeling studies. The structure reveals the phospho-specific interaction between RBM17 and ATXN1. Furthermore, we validated the structure and the interaction by mutagenesis study with SPR binding experiments. This work provides molecular understanding on the phospho-specific interaction of RBM17 toward ATXN1 implicated in SCA1 pathology.

2. Materials and methods

2.1. Molecular modeling

To predict the complex structure of RBM17 and the phosphorylated ATXN1 (pATXN1) 6mer peptide, molecular modeling studies were conducted using the X-ray crystal structure of RBM17 complexed with ULM5 peptide (PDB code: 2PEH) [17]. The protein structure was cleaned up, and the 3D structure of the peptide was generated by Concord and energy minimized using MMFF94s force field and MMFF94 charges in Tripos SYBYL-X2.0. The flexible docking was carried out using GOLD v5.0.1 with the binding site defined as 10 Å around the co-crystallized ULM5 peptide. The ligand was docked using the similarity, region, and H-bond constraints, and evaluated by the GoldScore scoring function. The computational calculations were undertaken on an Intel® Xeon™ Quad-core workstation with Linux Cent OS release 5.5.

2.2. Protein expression and purification

All proteins were expressed using *Escherichia coli* BL21 (DE3) cell line at 18 °C with 1 mM isopropyl β-D-1-thiogalactopyranoside, and purified by Ni–NTA (Qiagen) affinity chromatography followed by HiTrapQ (GE healthcare) anion-exchange and Superdex75 (GE healthcare) size exclusion chromatography. All mutants were generated using Quick Change Site-directed mutagenesis kit (Stratagen).

2.3. Surface plasmon resonance (SPR)

All interactions between RBM17 and ATXN1 were measured by Surface Plasmon Resonance technique using Biacore 3000 or T200 (GE Healthcare). A running buffer composed of 150 mM NaCl, 10 mM HEPES PH7.4, 3 mM EDTA and 0.005% (v/v) Tween20 was used for all experiments and a buffer containing 1 M NaCl or 2 M NaCl, 10 mM HEPES pH 7.5, 3 mM EDTA, and 0.005 % (v/v) Tween 20 was used as a regeneration buffer. The data were analyzed using Bia Evaluation software (GE Healthcare).

3. Results

3.1. Prediction of the ATXN1 and RBM17 complex structure

The polyglutamine-expanded ATXN1 preferentially interacts with RBM17, and the phosphorylation of Ser776 in ATXN1 is shown to be critical for the binding to this partner protein [7,15]. In order to predict the complex structure of the phosphorylated ATXN1 (pATXN1) and RBM17, molecular modeling studies were performed. It was reported that RBM17 (a.k.a SPF45) can bind to both ATXN1 and ULM5, and their binding motifs have high sequence similarity (Fig. 1A) [17]. Therefore, the X-ray crystal structure of RBM17 (301–401 a.a.) complexed with ULM5 peptide (PDB code: 2PEH) was used for the modeling of pATXN1–RBM17 complex structure. We focused on the region where ULM5 peptide demonstrated the tight interactions with RBM17 (see the region within the double-ended arrow in Fig. 1A), and the co-crystallized ULM5 6mer peptide was modified to pATXN1 6mer (RRWpSAP). Then, flexible docking of pATXN1 peptide onto RBM17 was carried out, and the resulting complex structure was further refined by the energy minimization.

The complex structure shows that pATXN1 6mer peptide binds tightly to RBM17 through the strong hydrophobic interactions and intensive salt-bridge/H-bonding network (Fig. 1B and E). Also, their overall structures show very good shape complementarities. Especially, $Trp775^{pATXN1}$ nicely occupies the deep hydrophobic pocket (Fig. 1C and D), which is formed by the helices αA and αB along with the hydrophobic side chains on the β-sheets of RBM17 (Fig. 1B) [17]. It makes the strong hydrophobic interactions with the surrounding residues, i.e., Phe377, Leu372, Val382, and Met312 of RBM17. Also, the NH moiety of the $Trp775^{pATXN1}$ indole ring forms the H-bond with $Glu325^{RBM17}$ (Fig. 1E). The residues located at the tip of the β-hairpin formed by the strands β3' and β4 of RBM17 [17], i.e., Arg375, Tyr376, and Phe377, appear to contribute to the binding with pATXN1. $Phe377^{RBM17}$ makes an orthogonal π–π stacking interaction with $Trp775^{pATXN1}$ and stacks with the alkyl group of $Arg774^{pATXN1}$. This threefold stacking among $Trp775^{pATXN1}$, $Phe377^{RBM17}$, and $Arg774^{pATXN1}$ stabilizes the complex structure of RBM17 and pATXN1. The backbone amide and carbonyl groups of $Tyr376^{RBM17}$ and $Gly379^{RBM17}$ make a hydrogen bonding with the backbone of the pATXN1 peptide. Interestingly, the guanidyl group of $Arg375^{RBM17}$ makes a strong salt-bridge interaction with the phosphorylated $Ser776^{pATXN1}$, and $Arg375^{RBM17}$ is stabilized by another salt-bridge with the carboxylate group of $Glu329^{RBM17}$. This tight interaction network among phospho-$Ser776^{pATXN1}$, $Arg375^{RBM17}$ and $GLu329^{RBM17}$ reflects that the interaction of ATXN1 and RBM17 requires the phosphorylation of this $Ser776^{pATXN1}$ residue [15]. Compared with the interactions of ULM5 peptide bound in RBM17, pATXN1 peptide makes additional strong H-bonding network with RBM17 using $Arg773^{pATXN1}$ residue. It is notable that the corresponding residue in ULM5 is Ser336 as shown in Fig. 1A. The guanidyl group of $Arg773^{pATXN1}$ interacts with the backbone carbonyl of $Glu325^{RBM17}$ and the carboxylate of $Glu329^{RBM17}$. This $Glu329^{RBM17}$ residue on the helix αA makes the salt-bridge interaction with $Arg375^{RBM17}$ in β3′ and stabilizes RBM17. At the end of the helix αA, the carboxylate groups of $Asp319^{RBM17}$ and $Glu325^{RBM17}$ form the salt–bridge interactions with $Arg774^{pATXN1}$. Altogether, molecular modeling results demonstrate that pATXN1 tightly binds to RBM17 with the strong electrostatic and hydrophobic interactions as well as good shape complementarities.

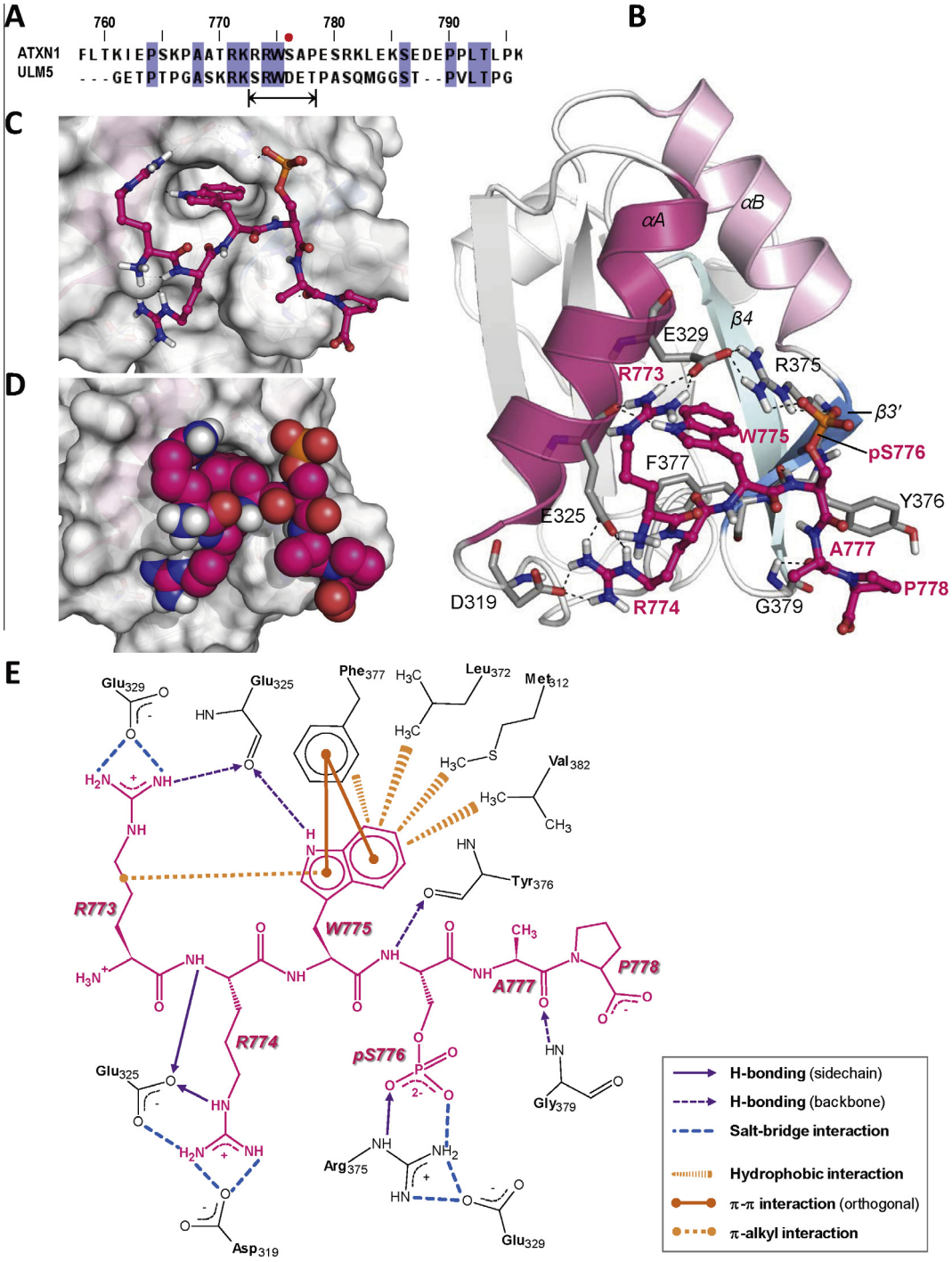

Fig. 1. Binding mode of pATXN1 6mer peptide in RBM17. Sequence alignment of ATXN1 and SF3b155-ULM5. The region where ULM5 makes tight interactions with RBM17 is marked within the double-ended arrow. The red dot above the sequence indicates Ser776 (A). Interactions between pATXN1 peptide and RBM17. The secondary structure of RBM17 is displayed in ribbon, and the helices αA (321–333) and αB (362–372), sheets β3′ (375–377) and β4 (380–387) are colored in pink, light-pink, skyblue, and pale blue, respectively. The RBM17 residues interacting with pATXN1 peptide are displayed in sticks with the carbon atoms in gray. The hydrogen bonds are marked with black dashed lines. The bound pATXN1 peptide is represented as ball-and-sticks with the carbon atoms in magenta, and the non-polar hydrogens are undisplayed for clarity (B). Tightly bound pATXN1 6mer peptide in the deep hydrophobic pocket of RBM17. The surface of RBM17 was colored in white (C). Shape complementarities between pATXN1 peptide and RBM17. The surface of RBM17 was displayed, and the bound pATXN1 peptide is represented as spheres with the carbon atoms in magenta (D). Schematic diagram of the interaction between pATXN1 peptide and RBM17. The structure of the pATXN1 6mer peptide is colored in magenta, and the interacting residues in RBM17 are in black. The interaction types are described in the gray box (E).

3.2. Binding analysis of ATXN1 and RBM17

The previous *in vivo* studies show that the phosphorylation of Ser776 of ATXN1 is essential for RBM17 binding [7,16]. Furthermore, the modeled structure of pATXN1–RBM17 shows that the phospho group of $pSer776^{ATXN1}$ interacts with RBM17 with a tight salt-bridge network. Therefore, to confirm that the phosphorylation of Ser775 in ATXN1 is important for the binding, the phosphorylation dependency of ATXN1–RBM17 interaction was examined by SPR. Since it is not practically feasible to make phosphorylated form of ATXN1, we decided to use a Ser776Asp mutant (AXH-RD) of ATXN1 (563–816 a.a.) as a phospho-mimic form of

ATXN1 encompassing from AXH domain to the end, while AXH-RS as an unphosphorylated form (Fig. 2A). We immobilized RBM17 on a CM5 sensor chip, and AXH-RD or AXH-RS was injected as analytes. Consistent with the previous study and our modeled structure, AXH-RS, an unphosphorylated form of ATXN1, shows little binding to RBM17, while AXH-RD, a mimic of phosphorylated form of ATXN1, shows high affinity binding to RBM17 with submicromolar range of K_D, which is estimated by fitting Sensorgram by Biaevaulation program (GE healthcare). With this platform, which enables us to investigate the interaction between the phosphorylated form of ATXN1 and RBM7, we further examined the binding between RBM17 and ATXN1 guided by the modeled structure. First, we mutagenized Arg375^{RBM17} to Lys, which is forming a tight salt-bridge network with the phosphor group of pSer776^{ATXN1} and Glu329^{RBM17}. Arg375Lys mutant would maintain alkyl group of the side chain as well as partial charge, while disrupting a tight salt-bridge with pS776^{ATXN1} and Glu329^{RBM17}. Therefore, this mutant will not disrupt the global structure of RBM17. We then measured its binding to AXH-RD with SPR. AXH-RD was immobilized on a CM5 sensor chip with 400 RU, and the wild-type or mutant RBM17 were injected as analytes in several different concentrations (0, 100, 500, 1000, 2000, and 5000 nM). SPR sensorgram in Fig. 2B shows that the wild-type RBM17 binds to AXH-RD with submicromolar range of K_D, while mutating Arg375 to Lys (RBM17$_{R375K}$) disrupts its binding ability to AXH-RD indicating that the salt-bridge network is critical for the interaction between RBM17 and the phosphorylated form of ATXN1 (Fig. 2B). We then further mutagenized Glu329^{RBM17} to Ala (RBM17$_{E329A}$) and measured its binding to AXH-RD. This mutant would disrupt the salt-bridge network at pSer776^{ATXN1} residue, but also disrupt the salt-bridge with Arg773^{ATXN1} (Fig. 1E). The fact RBM17$_{E329A}$ mutant lost its binding ability toward RBM17 further supports that the salt-bridge network is essential for the interaction between RBM17 and ATXN1.

The modeled structure reveals that Arg773^{ATXN1} makes a salt-bridge with Glu329^{RBM17}, which is not present in RBM17-ULM5 interaction (Fig. 1A and B). Arg773^{ATXN1} is evolutionarily conserved among species. Therefore, we decided to evaluate the contribution of Arg773^{ATXN1} in its binding to RBM17. We generated two ATXN1 mutants: AXH-SD containing Arg773Ser mutation and the phospho-mimic Ser776Asp mutation, and AXH-SS containing Arg773-Ser mutation and Ser776 as an unphosphorylated form. The binding between these two mutants and RBM17 were then measured by SPR. AXH-SD shows significantly lower binding affinity to RBM17 than AXH-RD, and AXH-SS shows almost no binding to RBM17. These data further support the modeled structure showing that the salt-bridge between Glu329^{RBM17} and Arg773^{ATXN1} contribute to the interaction between ATXN1 and RBM17 (Fig. 2B). Considering that the Arg773^{ATXN1} equivalent residue of ULM5 is Ser and that Arg773Ser ATXN1 mutant shows lower binding affinity than ATXN1 wild-type, RBM17 may prefer ATXN1 to ULM5 in its binding. In addition, we generated RBM17$_{F377A}$ mutant. As the modeled structure shows that Phe377^{RBM17} plays a central role in accommodating pATXN1, the Phe337Ala RBM17 mutant abrogates its binding ability to AXH-RD. With the modeled structure, these data reveal that the phosphorylation of Ser776^{ATXN1} is a major contributor to RBM17 binding, and Arg773^{ATXN1} also contributes to interaction with RBM17. In order to obtain further insights into the interaction between ATXN1 and RBM17, we decided to examine whether the outside of the phosphorylated Ser776 region in ATXN1 is involved in interacting with RBM17. First, we deleted the C-terminal region in the phosphorylated form (AXH-RD$_{\Delta 779-816}$) or in the wild-type (AXH-RS$_{\Delta 779-816}$), and measured the binding with RBM17 (Fig. 2C). AXH-RD$_{\Delta 779-816}$ shows almost identical binding kinetics with that of AXH-RD with the phosphorylation dependency. This data indicate that the C-terminal region juxtaposed to the RBM17 binding site is not involved in RBM17 interaction.

Since the AXH domain forms a homodimer and the AXH domain might affect the binding of RBM17, we decided to delete the AXH domain (RD$_{\Delta AXH\ \Delta 779-816}$ or RS$_{\Delta AXH\ \Delta 779-816}$) on the addition with the C-terminal deletion, and examined their bindings with RBM17 (Fig. 2C). Although RD$_{\Delta AXH\ \Delta 779-816}$ without the AXH domain shows faster association and dissociation than AXH-RD domain, the phosphorylation dependency of the binding were maintained in RD$_{\Delta AXH\ \Delta 779-816}$ or RS$_{\Delta AXH\ \Delta 779-816}$. The different binding kinetics between AXH-RD and RD is probably due to the absence of the AXH domain making the analyte as monomer, but not because of the contribution of the AXH domain to its bindings, as we have not observed the direct binding between AXH domain and RBM17 (data not shown).

Our previous structural study on ATXN1–CIC complex showed that ATXN1 homodimer is disrupted upon CIC binding to make a new form of ATXN1–CIC tetramer [12]. Having that ATXN1 interacts with both CIC and RBM17, we decided to examine whether the ATXN1–CIC tetramer form is also competent for RBM17 binding. We generated the tetramer form of ATXN1–CIC complex by incubating AXH-RD with CIC$_{28}$ peptide (MFVWTNVEPRSVAVFPWHSLVPFLAPSQ) and the AXH-RD/CIC$_{28}$ complex formation was monitored by a native PAGE gel (Fig. 2D). We then compared the binding abilities between AXH-RD and AXH-RD/CIC$_{28}$ toward RBM17 by SPR. Fig. 2D shows that AXH-RD/CIC28 and AXH-RD alone show similar binding for RBM17. This data suggest that the AXH-RD-CIC$_{28}$ tetramer complex formation does not affect the binding ability of ATXN1 to RBM17.

4. Discussion

This work provides the structural and molecular basis of the phosphorylation dependency of ATXN1 binding to RBM17. RBM17 is a splicing factor interacting with the 3′ splice site recognizing factors U2AF65, SF1 and SF3b155. RBM17 is also identified as a binding partner of ATXN1 preferentially with the polyglutamine expanded form of ATXN1 and this interaction has been implicated with SCA1 pathology [7]. MSK1 phosphorylates Ser776 of ATXN1 and the Ser776 phosphorylation is required for RBM17 binding. The modeled structure of pATXN1 peptide and RBM17 reveals that a tight salt-bridge network confers the phosphorylation dependency of ATXN1 binding to RMB17. Interestingly, the pSer776^{ATXN1} equivalent residue in ULM5 is Asp339^{ULM5}, and the carboxylate of Asp339^{ULM5} side chain is also making a tight salt-bridge network with RBM17 indicating that RBM17 recognizes pSer776^{ATXN1} residue in the same manner with Asp339^{ULM5}. This observation attests that a phosphorylated Ser binding pocket can accommodates an Asp residue. The modeled structure also shows the ATXN1-unique interaction with RBM17, which was not observed in ULM5 binding. Arg773^{ATXN1} forms a salt-bridge with Glu329^{RBM17}. When Arg773^{ATXN1} to Ser mutant, which is the equivalent amino acid of ULM5, shows significantly lower binding than the wild-type, suggesting that this interaction may be a key for RBM17 to distinguish between ATXN1 and ULM5. A previous study shows that ATXN1–RBM17 and ATXN1–CIC complexes seem to be distinct and mutually exclusive *in vivo* [7]. However, our data shows that ATXN1–CIC peptide complex is capable of binding to RBM17. This observation raises interesting possibilities. Considering that CIC is a relative large protein (>160 KDa) and we used CIC$_{28}$ peptide to induce ATXN1–CIC hetero-tetramerization, the complex formation of ATXN1 and full-length CIC might affect the binding capability toward RBM17 generating distinct complexes. Alternatively, the

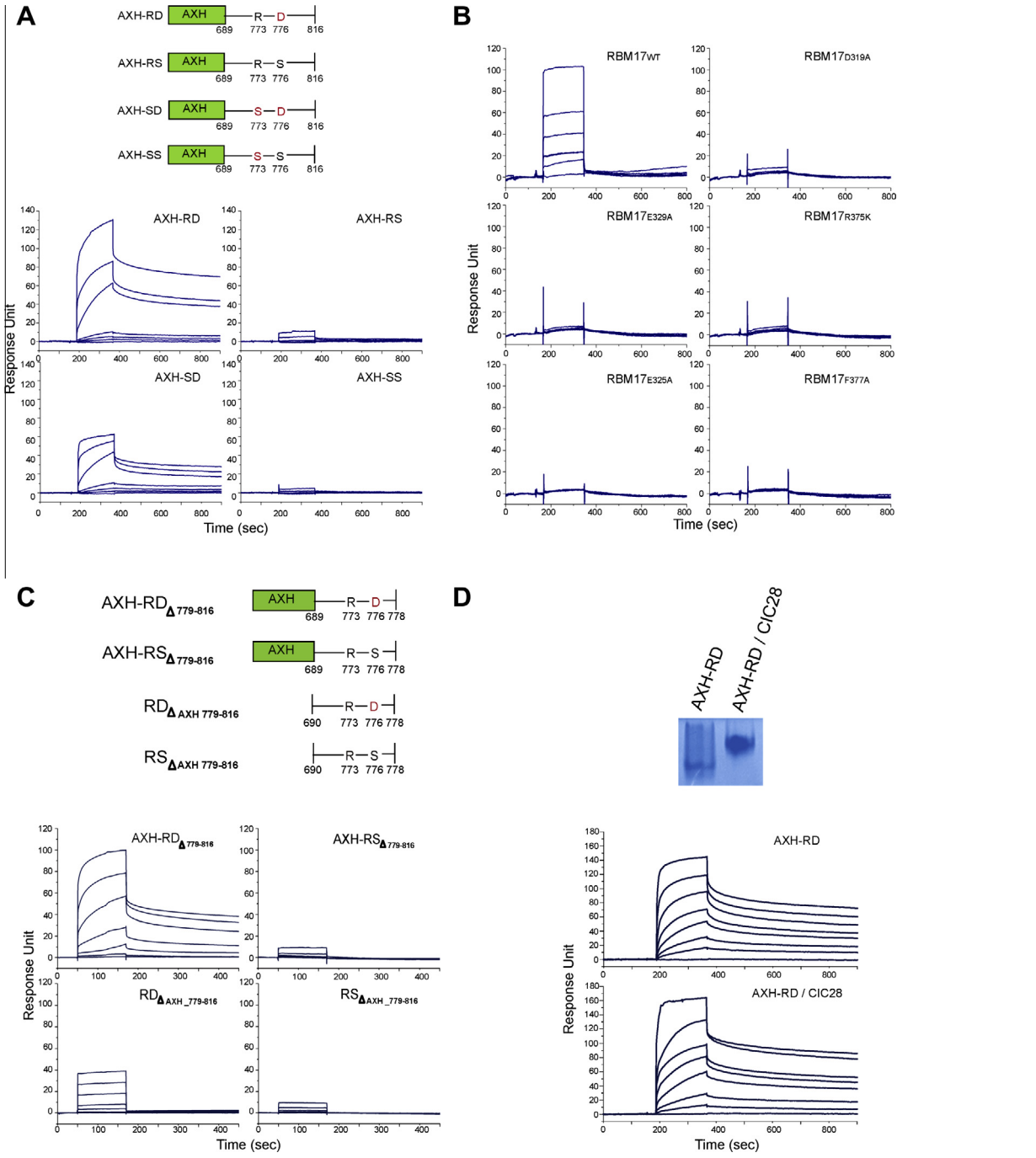

Fig. 2. Surface plasmon resonance analysis of ATXN1 and RBM17 interaction. SPR binding analysis of ATXN1 and RBM17. The upper panel shows the constructs used in this SPR experiments. The lower panel shows SPR sensorgram. RBM17 was immobilized on a CM5 sensor chip (141 RU) and AXH-RD, AHX-RS, AXH-SD, AXH-SS were used as analytes (0, 15.63, 31.25, 62.5, 250, 1000 and 2000 nM) (A). SPR binding analysis of ATXN1 and RBM17 mutants. AXH-RD was immobilized on a CM5 sensor chip (400 RU). RBM17 mutants were injected as analytes (0, 100, 500, 1000, 2000, 5000 nM) (B). SPR binding analysis between RBM17 and AXH-RD, AXH-RS and their deletion constructs. RBM17 were immobilized on a CM5 sensor chip (93.4 RU) and ATXN1 constructs (0, 62.5, 125, 250, 500, 1000, 2000, and 4000 nM) (C). SPR binding analysis of AXH-RD and AXH-RD/CIC_{28}. AXH-RD/CIC_{28} tetramer formation was shown in a native PAGE (upper panel). RBM17 were immobilized on a CM5 sensor chip (99.8 RU) and AXH-RD and AXH-RD/CIC_{28} were used as analytes (0, 31.25, 62.5, 125, 250, 500, 1000, and 2000 nM) (D).

ATXN1 complex with full-length CIC might still maintain its binding ability with RBM17, but the distinct complexes shown *in vivo* might be due to different localizations of CIC and RBM17. Overall, this work provides the structural and molecular basis of the interaction between RBM17 and the phosphorylated form of ATXN1. Furthermore, the structure of RBM17 and pATXN1 peptide might be utilized to target RBM17–pATXN1 interaction to modulate SCA1 pathogenesis.

Acknowledgments

This work was supported by the grants from National Leading Research Lab (NLRL) program (2011-0028885) to S. Choi; and grants (NRF-2013R1A1A2055605, NRF-2011-0031416, 2011-0020334, 2011-0031955) to J.-J. Song through the Ministry of Science, ICT & Future Planning (MSIP) and National Research Foundation (NRF) of Korea.

References

[1] B.E. Riley, H.T. Orr, Polyglutamine neurodegenerative diseases and regulation of transcription: assembling the puzzle, Genes Dev. 20 (2006) 2183–2192.

[2] H.Y. Zoghbi, M.S. Pollack, L.A. Lyons, R.E. Ferrell, S.P. Daiger, A.L. Beaudet, Spinocerebellar ataxia: variable age of onset and linkage to human leukocyte antigen in a large kindred, Ann. Neurol. 23 (1988) 580–584.

[3] C.J. Cummings, H.T. Orr, H.Y. Zoghbi, Progress in pathogenesis studies of spinocerebellar ataxia type 1, Philos. Trans. R. Soc. Lond. B Biol. Sci. 354 (1999) 1079–1081.

[4] A.H. Koeppen, The pathogenesis of spinocerebellar ataxia, Cerebellum 4 (2005) 62–73.

[5] S. Banfi, A. Servadio, M.Y. Chung, T.J. Kwiatkowski Jr., A.E. McCall, L.A. Duvick, Y. Shen, E.J. Roth, H.T. Orr, H.Y. Zoghbi, Identification and characterization of the gene causing type 1 spinocerebellar ataxia, Nat. Genet. 7 (1994) 513–520.

[6] H.T. Orr, M.Y. Chung, S. Banfi, T.J. Kwiatkowski Jr., A. Servadio, A.L. Beaudet, A.E. McCall, L.A. Duvick, L.P. Ranum, H.Y. Zoghbi, Expansion of an unstable trinucleotide CAG repeat in spinocerebellar ataxia type 1, Nat. Genet. 4 (1993) 221–226.

[7] J. Lim, J. Crespo-Barreto, P. Jafar-Nejad, A.B. Bowman, R. Richman, D.E. Hill, H.T. Orr, H.Y. Zoghbi, Opposing effects of polyglutamine expansion on native protein complexes contribute to SCA1, Nature 452 (2008) 713–718.

[8] H.T. Orr, SCA1-phosphorylation, a regulator of Ataxin-1 function and pathogenesis, Prog. Neurobiol. 99 (2012) 179–185.

[9] C.J. Lee, W.I. Chan, M. Cheung, Y.C. Cheng, V.J. Appleby, A.T. Orme, P.J. Scotting, CIC, a member of a novel subfamily of the HMG-box superfamily, is transiently expressed in developing granule neurons, Brain Res. Mol. Brain Res. 106 (2002) 151–156.

[10] C.J. Lee, W.I. Chan, P.J. Scotting, CIC, a gene involved in cerebellar development and ErbB signaling, is significantly expressed in medulloblastomas, J. Neurooncol. 73 (2005) 101–108.

[11] J.D. Fryer, P. Yu, H. Kang, C. Mandel-Brehm, A.N. Carter, J. Crespo-Barreto, Y. Gao, A. Flora, C. Shaw, H.T. Orr, H.Y. Zoghbi, Exercise and genetic rescue of SCA1 via the transcriptional repressor Capicua, Science 334 (2011) 690–693.

[12] E. Kim, H.C. Lu, H.Y. Zoghbi, J.J. Song, Structural basis of protein complex formation and reconfiguration by polyglutamine disease protein Ataxin-1 and Capicua, Genes Dev. 27 (2013) 590–595.

[13] M.J. Lallena, K.J. Chalmers, S. Llamazares, A.I. Lamond, J. Valcarcel, Splicing regulation at the second catalytic step by sex-lethal involves 3′ splice site recognition by SPF45, Cell 109 (2002) 285–296.

[14] L. Duvick, J. Barnes, B. Ebner, S. Agrawal, M. Andresen, J. Lim, G.J. Giesler, H.Y. Zoghbi, H.T. Orr, SCA1-like disease in mice expressing wild-type ataxin-1 with a serine to aspartic acid replacement at residue 776, Neuron 67 (2010) 929–935.

[15] E.S. Emamian, M.D. Kaytor, L.A. Duvick, T. Zu, S.K. Tousey, H.Y. Zoghbi, H.B. Clark, H.T. Orr, Serine 776 of ataxin-1 is critical for polyglutamine-induced disease in SCA1 transgenic mice, Neuron 38 (2003) 375–387.

[16] J. Park, I. Al-Ramahi, Q. Tan, N. Mollema, J.R. Diaz-Garcia, T. Gallego-Flores, H.C. Lu, S. Lagalwar, L. Duvick, H. Kang, Y. Lee, P. Jafar-Nejad, L.S. Sayegh, R. Richman, X. Liu, Y. Gao, C.A. Shaw, J.S. Arthur, H.T. Orr, T.F. Westbrook, J. Botas, H.Y. Zoghbi, RAS-MAPK-MSK1 pathway modulates ataxin 1 protein levels and toxicity in SCA1, Nature 498 (2013) 325–331.

[17] L. Corsini, S. Bonnal, J. Basquin, M. Hothorn, K. Scheffzek, J. Valcarcel, M. Sattler, U2AF-homology motif interactions are required for alternative splicing regulation by SPF45, Nat. Struct. Mol. Biol. 14 (2007) 620–629.